Available online at www.sciencedirect.com
SCIENCE DIRECT®
European Journal of Mechanics B/Fluids 24 (2005) 353–365

Transitional flow field characterization inside an arteriovenous graft-to-vein anastomosis under pulsatile flow conditions

Nurullah Arslan [a,*], Francis Loth [b], Christopher D. Bertram [c], Hisham S. Bassiouny [d]

[a] *Fatih University, Industrial Engineering Department, Istanbul, Turkey*
[b] *The University of Illinois at Chicago, Department of Mechanical and Industrial Engineering, Chicago, USA*
[c] *University of South Wales, Biomedical Engineering Department, South Wales, Australia*
[d] *University of Chicago, Surgery Department, Chicago, USA*

Received 13 November 2003; received in revised form 5 April 2004; accepted 20 September 2004

Available online 30 October 2004

Abstract

The objective of this study was to investigate the relationship between the distribution of turbulence intensity and the localization of stenoses inside the venous anastomosis of arteriovenous (AV) grafts. Turbulent flow measurements were conducted inside an upscaled end-to-side graft model under pulsatile flow conditions. The pulsatile flow waveforms had maximum, minimum and mean Reynolds numbers of 2500, 1200 and 1800, respectively based on the graft diameter. The distribution of the velocity and turbulence intensity was measured at several locations in the plane of the bifurcation of the model. Turbulence intensity was found to be greatest downstream of the anastomosis. Results indicate a possible relation between the vein wall and graft vibration and the development of intimal hyperplasia which is correlated with the animal studies cited in the paper. Future studies are required to better understand the mechanism of formation of the intimal hyperplasia and the level of the turbulence.

Keywords: Arteriovenous graft; Dialysis; Turbulence; Laser Doppler anemometer; Stenosis

1. Introduction

Computational [1,2] and experimental [3–5] investigations of the fluid dynamics of distal end-to-side anastomoses associated with arterial bypass grafts have been conducted, motivated by the fact that this junction is a site of particularly high risk in intimal hyperplasia and other forms of arterial disease. A further motivation is that the junction offers a situation providing a complex mix of fluid dynamic phenomena and can potentially aid the quest for causal linkages between disease localization and fluid dynamic details for arteries in general.

A similar geometry occurs at the downstream end of an arteriovenous anastomosis created by incorporation of a loop of graft material for the purposes of repeated high-flow-rate vascular access, as in renal dialysis. Similar experiences of intimal hyperplasia leading to loss of patency, but now in the vein rather than the downstream artery, have as in the arterial bypass graft situation led surgeons to experiment with a variety of detailed geometries when forming the end-to-side anastomosis between

* Corresponding author. Tel: +90 212 8890837; fax: +90 212 8891142.
E-mail address: narslan@fatih.edu.tr (N. Arslan).

0997-7546/$ – see front matter
doi:10.1016/j.euromechflu.2004.09.004

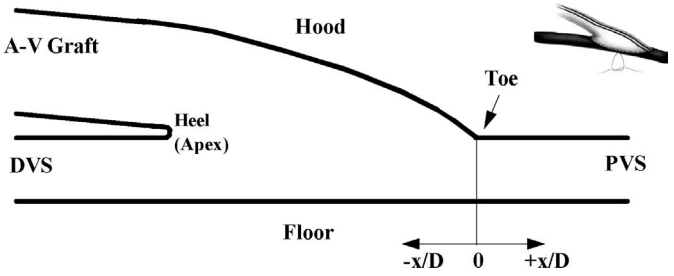

Fig. 1. Geometry and nomenclature of the venous anastomosis of an A-V graft model.

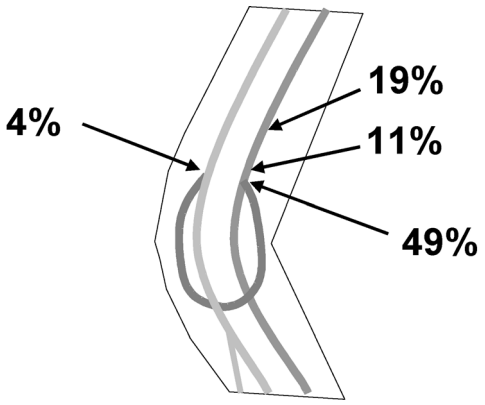

Fig. 2. Distribution of hyperplastic stenoses according to Kanterman et al. [6].

the graft and the vein. Kanterman [6] have shown that hyperplastic stenoses occur predominantly in the proximal venous segment (PVS), downstream of the graft-to-vein junction, as shown in Fig. 1. Distribution of hyperplastic stenoses according to Kanterman et al. is shown in Fig. 2. This suggests the possible involvement of disturbances to flow created in the graft-to-vein junction and advected downstream.

Shu et al. [7] obtained the mean velocity profiles and wall shear stresses (WSS) inside realistic AV graft models. They implicated the low and oscillating WSS near the stagnation point and separation region in the development of a lesion distal to the toe (see Fig. 1). No measurements of turbulence levels were reported.

The first in vitro modeling study was done on the turbulence measurements quantitatively by Arslan and Loth et al. [8,9]. The location of the WSS and turbulence regions inside an AV graft model under steady flow conditions were investigated experimentally using laser Doppler anemometer and computationally using spectral element technique [9,10].

Fillinger et al. [11–13] used canine in vivo flow models to examine the importance of turbulence on intimal growth at the venous anastomosis. Turbulence was accessed by measuring tissue vibration. The AV graft consisted a femoral artery connected to the femoral vein with a polytetrafluoroethylene (PTFE) graft of length 25 cm. They used three different grafts untapered 6-mm grafts, 4 to 7-mm tapered grafts and 7 to 4-mm tapered grafts. Flow rates ranging from 462 ± 25 to 1340 ± 140 ml/min were determined by electromagnetic flowmeter (Caroline Medical Electronics, King, N.C.) and transit-time ultrasound flowmeter (Transonic Systems Inc., Ithaca, N.Y.) to produce a wide range of flow conditions, including laminar and turbulent flow. As the flow rates increased, the visual signs of flow disturbances or turbulence increased. At higher flow rates the flow disturbances were severe enough to cause rapid movements or vibrations of the vessel wall and perivascular tissue. Level of vibration was measured by color Doppler ultrasound imaging. Color Doppler ultrasound imaging displayed the movement as a color map by processing phase and frequency shift information from the reflected ultrasound. Perivascular tissue vibration at the venous anastomosis was thus demonstrated visually. By using standardized power, gain, and threshold settings, they compared vibration signals from one graft to another. By measuring the distance required for the signal to attenuate below a specified threshold (19 decibels), they quantified the volume of perivascular tissue vibration. They theorized that this volume of tissue vibration is related to the quantity of energy loss and the level of turbulence. In one canine study Fillinger et al. (1989) placed a Teflon tape just after the arterial anastomosis to create different levels of tissue vibration in two venous anastomoses. They found a greater degree of intimal-medial thickening in the anastomosis in which tissue vibration was more severe. They found tissue vibration to be most severe near the venous anastomosis. They concluded from their measurements that turbulence was a major

factor in the development of venous intimal-medial thickening in AV grafts. They also correlated Reynolds number with intimal thickening at the venous anastomosis.

While these studies have contributed to our understanding of the intimal hyperplasia formation in the anastomosis they did not fully take into account all of the special fluid mechanical circumstances pertaining to this junction. The major differences between these two end-to-side anastomoses, the arterial and the venous, from the fluid mechanical point of view, relate to the higher flow-rate. Higher flow-rate is a consequence of the fact that the arteriovenous shunt bypasses the peripheral resistance, forcing the heart to increase cardiac output by virtue of the increased venous return. Unlike the arterial bypass graft, where the predominant resistance is peripheral, and the graft therefore does not set its own flow-rate, the arteriovenous graft does; its own resistance determines the shunt flow.

Higher Reynolds number implies a greater tendency to flow instability and turbulence, as noted by Fillinger et al. [11–13]. Whereas the arterial bypass junction is unlikely to be turbulent, the venous one is more than likely to be. Evidence to support this reasoning is provided by the results of our own ultrasonic measurements of flow-rates and vessel diameters in a patient with such an arteriovenous graft, as reported below. We assume that turbulent flow is likely in any graft-to-vein junction having the diameter and flow-rate necessary for continuing patency and dialysis use.

The main goal of the present research is to investigate the possible relationship between turbulence level and AV graft failure. In this study, we report the experimental measurements under pulsatile flow conditions of the magnitude and spatial distribution of turbulence inside an in vitro graft model representative of the graft-to-vein junction of a dialysis AV graft.

2. Methods

2.1. In vivo measurements

AV graft-vein junction flow conditions and vessel diameters were determined using Color Doppler ultrasound measurements (Acuson 128XP/10) were conducted on two dialysis patients. The measurements were conducted within one month of graft construction. Fig. 3 shows the geometry (A) and B-scan-mode (B, C, D) outline of the venous anastomosis in one of the patients. The PTFE AV graft connected the brachial artery to the basilic vein near the patient's elbow. As seen in Fig. 3(A), the measured graft lumen diameter (D) for this patient was 6.0 mm; in the other patient it was 6.7 mm. In both patients, the PVS and distal vein segment (DVS) were of comparable diameter and somewhat smaller than the graft. The angle of between the graft and the vein was 45° in one patient and much smaller in the patient shown in Fig. 3. There is considerable variation in the geometry from patient to patient for surgical reasons.

For the patient shown in Fig. 3, the instantaneous mean of the sonograph trace was estimated to be 1.5 m/s at the maximum and 1.0 m/s at the minimum of the cycle. For the other patient, the corresponding numbers were 1.2 and 0.8 m/s. Measurements were also made in the PVS and DVS; however, determination of the mean velocity was difficult because of the degree of spectral broadening. Reynolds numbers for the graft are difficult to estimate, since the shape of the velocity profile is unknown and the sample volume did not cover the whole vessel lumen. Based on the velocity measured in the sample volume (V), and assuming normal blood viscosity ($\mu = 3.5$ mPa s), the above measurements lead to a systolic peak Reynolds number of 2700 and a diastolic minimum of 1800 for the patient shown in Fig. 3 ($Re = \rho V D/\mu$, where $\rho =$ blood density, 1.05 g/ml, $D =$ vein diameter). For the other patient, the corresponding values are 2400 and 1600. Two assumptions are here implicit: (1) that the velocity profile is flat, and (2) that the patient has normal haematocrit. The true in vivo Reynolds number therefore remains unknown; however, the range appears to span the critical number for transition to turbulence in a circular pipe ($Re_{\text{critical}} \approx 2300$).

2.2. Model geometry

The anastomosis model used in this study was that previously used by Loth [5] to investigate the haemodynamics in a distal end-to-side arterial bypass anastomosis. This model geometry also closely approximates the graft-vein junction of the A-V graft. The model was scaled up eight times relative to the in vivo case. The model material was a transparent elastomer (Sylgard 184, Dow Corning), and the walls were thick enough that the model could be considered essentially rigid. The graft-to-vein diameter ratio was 1.6, with a graft lumen diameter of 50.8 mm and a host vein diameter of 31.75 mm. The graft axis intersected the host vein axis at an angle of 5°.

2.3. In vitro measurements

2.3.1. Flow system and flow rate for pulsatile flow

An experimental system was designed and constructed to provide the upscaled model with the proper inlet and outlet flow conditions Arslan [8]. The fluid employed, a mixture of 42% water and 58% glycerine by weight, was chosen to match the

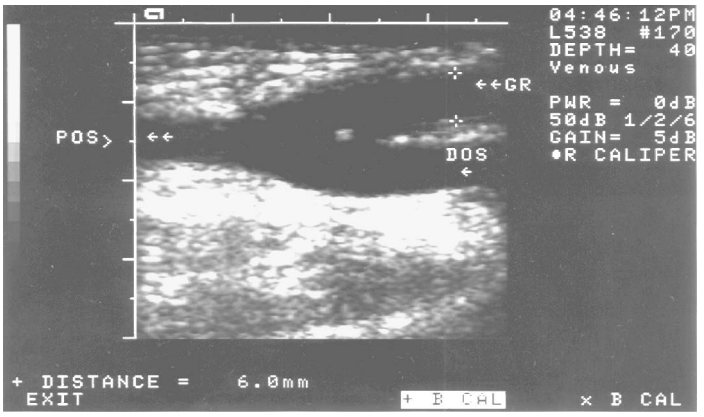

(A)

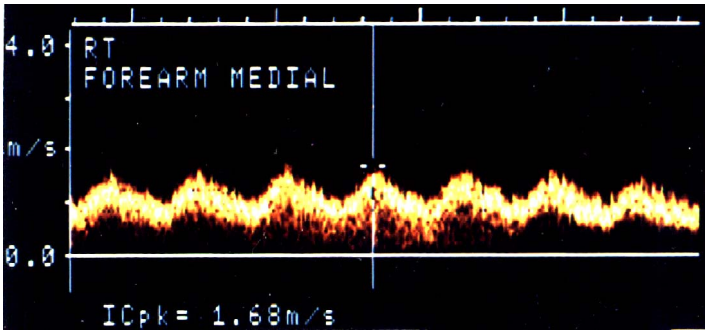

(B)

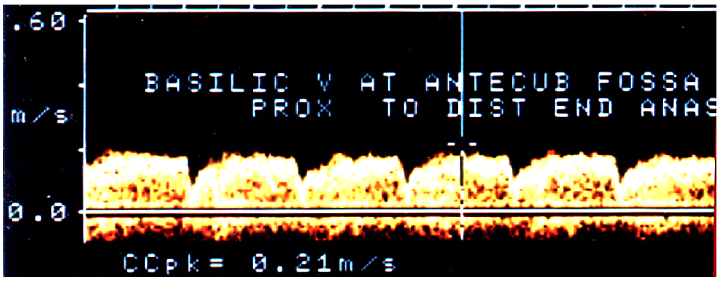

(C)

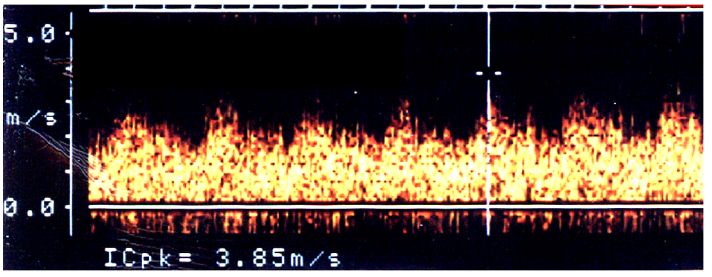

(D)

Fig. 3. Geometry (A) and ultrasonic B-mode scans of a dialysis patient's graft-to-vein junction (venous anastomosis) inside (B) graft (C) Distal vein segment (PVS), (D) proximal vein segment (DVS) [9].

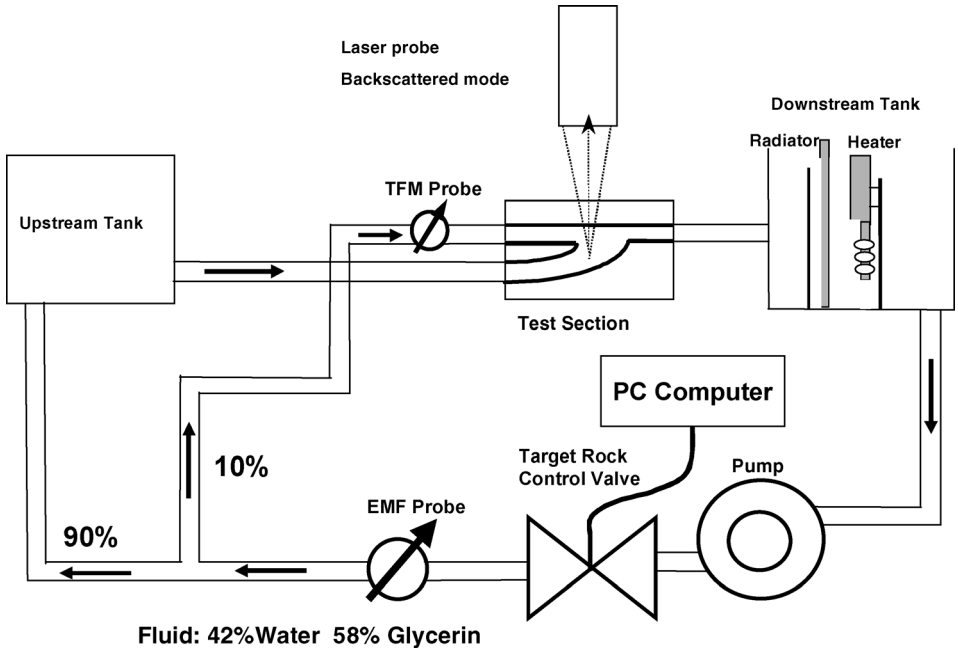

Fig. 4. Experimental flow system [8].

index of refraction of the Sylgard model ($n = 1.41$). This fluid had a refractive index of 1.41, a density of 1.16 g/ml, and a dynamic viscosity of 10-mPa s as measured by a Wells-Brookfield LVTDV-II spindle type micro-viscometer at 25 °C. A 1/3 HP centrifugal Teel split-phase pump provided the pressure head to drive the flow. The total flow-rate was measured by bucket and stopwatch. Clinical experience is that the vein distal to the graft-vein junction often occludes; when it remains patent the flow-rate is typically small (less than 10% of the total flow-rate into the venous anastomosis). The ratio of the graft inlet flow-rate to the DVS inlet flow-rate was here chosen to be 90:10. The DVS inlet flow-rate was measured by an ultrasound transit-time flowmeter (Transonic model T101). Since fluid viscosity depends sensitively on temperature, a heater/mixer in the downstream tank was used to keep the fluid temperature at 23 ± 0.5 °C during the experiments. The flow system is shown in Fig. 4. The model was placed in a flow circuit under pulsatile flow conditions such that flow entered the graft from a straight tube four meters long with an inner diameter of 50.8 mm.

2.3.2. Laser doppler anemometry

Velocity profiles were obtained by measuring the particle velocities at the millimeter-spaced points along the bifurcation plane. Thirteen axial locations along the vein axis were examined, starting distally (upstream) at $X = -6.8D$ relative to the toe position, and extending proximally to $X = +3.6D$. The two components of velocity were measured simultaneously with a two-color laser system (DANTEC, mirror type F147/B073 model 5500A), which used a 350 mW argon-ion laser (blue = 488 nm, green = 514.5 nm). The two measured velocity components were in the plane of the bifurcation; the u-component was parallel to the vein axis and the v-component was perpendicular to it. The system consists of two Bragg cells, two photomultipliers with receiving optics and two electronic counters. The Bragg cells were included so that forward and reverse velocities could be detected. The particles used to scatter the laser light were 0.993 μm diameter polymer micro spheres (Duke Scientific Corporation, Palo Alto, CA, cat. no. 4009B). The turbulence fluctuations and Reynolds stresses were calculated as using a data processing algorithm for pulsatile flow [10]. All measurements were scaled to in vivo values ($V_{\text{vivo}} = 2.5V_{\text{vitro}}$).

2.3.3. Data processing

The data acquisition program (SIZEWARE) recorded the laser Doppler anemometer (LDA) Doppler burst frequencies and the signal processor (Dantec 50N10) converted these frequencies to velocities at a specific spatial location for 20 cycles with a period of 16 seconds. A measurement at one spatial location required twenty pulsatile flow cycles at a period of 16 seconds. The time period of 16 seconds was found by simulating the Womersley number ($\alpha = 5.2$ in the present experiment) for in vivo and in vitro cases. The Womersley number is $\alpha = R(2\pi f/\nu)^{1/2} = R(2\pi(1/T)/\nu)^{1/2}$ and time period in vitro $T_{\text{vitro}} = 2\pi R^2/\nu\alpha^2$. Where α, Womersley number, R, radius of the inlet tube (cm), f, frequency (BPM/60), ν, kinematic viscosity (cm^2/s). The

total time required for one measurement point was fifteen minutes for pulsatile flow which included time to move the LDA sample volume to the next position as well as processing and observing the results of the experiment.

The instantaneous velocity data from LDA measurements was first interpolated by a FORTRAN code which interpolated between random bursts to provide evenly spaced data (2048 points per cycle) [8]. The twenty cycles of evenly spaced data were ensemble averaged with the same program, and the data were than rearranged such that the temporal starting point was consistent for all data points. The velocity data file has 2048 points. The ensemble-averaged values were subtracted from each instantaneous value at each cycle for twenty cycles and fluctuation velocities and Reynolds stress were found from these results.

Ensemble-averaged velocities in x and y direction (u_{ens} and v_{ens})

$$u_{\text{ens}}(k) = \frac{\sum_{j=1}^{\text{Ncycle}} u(k,j)}{N_{\text{cycle}}}, \quad k = 1, 2, 3, \ldots, N_{\text{points}},$$

$$v_{\text{ens}}(k) = \frac{\sum_{j=1}^{\text{Ncycle}} v(k,j)}{N_{\text{cycle}}}, \quad k = 1, 2, 3, \ldots, N_{\text{points}}.$$

Where $N_{\text{points}} = 2048$, $N_{\text{cycle}} = 20$, k = numbers of the points in one cycle $= 1, 2, 3, \ldots, N_{\text{points}}$, j = numbers of cycle at each measurement point $= 1, 2, 3, \ldots, N_{\text{cycle}}$, $u(k, j)$ = instantaneous velocity at specified point.

Ensemble averaged fluctuation velocities in x and y direction (u'_{ens} and v'_{ens})

$$u'_{\text{ens}}(k) = \frac{\sum_{j=1}^{\text{Ncycle}} \text{sqrt}[(u(k,j) - u_{\text{ens}}(k))^2]}{N_{\text{cycle}}}, \quad k = 1, 2, 3, \ldots, N_{\text{points}},$$

$$v'_{\text{ens}}(k) = \frac{\sum_{j=1}^{\text{Ncycle}} \text{sqrt}[(v(k,j) - v_{\text{ens}}(k))^2]}{N_{\text{cycle}}}, \quad k = 1, 2, 3, \ldots, N_{\text{points}}.$$

Ensemble-averaged Reynolds stress ($\overline{u'v'}$)

$$\overline{u'v'} = \frac{\sum_{j=1}^{\text{Ncycle}} [u(k,j) - u_{\text{ens}}(k)][(v(k,j) - v_{\text{ens}}(k)]}{N_{\text{cycle}}}, \quad k = 1, 2, 3, \ldots, N_{\text{points}}.$$

The mean velocities, fluctuation velocities and Reynolds stress values for pulsatile flow at a specific location were found for one hundred twenty angles (120) from 2048 data points.

3. Results

Velocity and turbulence measurements were performed at the midplane of the AV graft model with a flow ratio of 90:10. The pulsatile flow waveforms had maximum, minimum and mean Reynolds numbers of 2500, 1200 and 1800, respectively based on the graft diameter. Equivalent instantaneous maximum, minimum and mean flow rates at these Reynolds numbers are 2080, 1008 and 1484 ml/min respectively.

Velocity measurements were made in the x and y directions giving the u and v components of velocity. The turbulence fluctuations and Reynolds stresses were calculated as using a data processing algorithm for pulsatile flow.

Fig. 5 shows flow rate versus phase angle, where Re_{30} refers to Reynolds number at phase angle of 30 degrees. Figs. 6–9 show the pulsatile flow field as vector and scatter plots at all specified positions in the cycle in order to present an overview of the measurement results. The phase positions and their corresponding instantaneous Reynolds numbers are systolic acceleration ($Re_{30} = 2000$), systolic peak ($Re_{60} = 2500$), systolic deceleration ($Re_{120} = 2300$) and diastole ($Re_{300} = 1250$) (see Fig. 5).

3.1. Systolic acceleration ($Re_{30} = 2000$)

Fig. 6(A) shows the vector plot at systolic acceleration. Flow enters the model from the graft with a fully developed blunt velocity profile with a centerline velocity of 152 cm/s at position $X = -6.6D$. Flow from the DVS was a parabolic velocity profile with centerline velocity of 43 cm/s. The flow entering from the graft merges with the flow entering from DVS. At position $X = -5.2D$, just before entering the anastomosis, the velocity profile slightly skewed towards the heel side of the graft. The heel side of the graft has a more favorable pressure gradient than the hood side, which causes the flow to be skewed toward the heel side. Inside the graft, flow expands to the larger area similar to a sudden expansion. The peak velocity maintains its magnitude as the flow moves proximally into the anastomosis. The flow accelerates proximally due to the reduction in cross sectional area. The velocity profiles in the entrance to the PVS are blunt near the floor side of PVS with high velocity

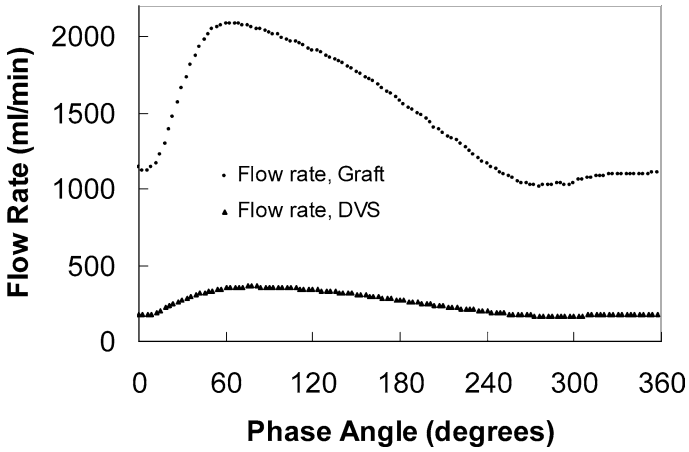

Fig. 5. Flow rate versus phase angles [8].

gradients near the wall and the v velocity component increases at the entrance of PVS. The value of the v_m increases from 130 to 217 cm/s between positions $X = -4.4D$ and $X = -0.4D$, respectively. A separation region downstream of the toe is evidenced by retrograde vectors near the wall at position $X = +0.4D$. The length of the separation region is estimated to be one diameter in length. The flow accelerates slightly near the center from 295 to 304 cm/s at positions $X = +0.4D$ to $X = +2.0D$, respectively. The velocity gradient on the toe side of the PVS increases significantly from position $X = +1.2D$ to $X = +3.6D$ in PVS. The small velocity gradient on the toe side of PVS shows low WSS on this side of PVS. The velocity vectors in PVS are parallel to the floor side that indicates weak secondary flow in PVS at this phase angle.

The turbulent fluctuations in both directions are given by Figs. 7(B)–(C). At the graft entrance u_{rms} profile is "M" shaped which is characteristic of transitional flow. The maximum fluctuation velocity at position $X = -6.6D$ was $u_{rms} = 7.8$ cm/s (5% of local mean velocity u_m) indicating low turbulence level at the graft inlet. The v_{rms} value was nearly zero. The turbulence level is almost the same magnitude inside the anastomosis up to the location of $X = +1.2D$ in PVS. It suddenly increases at position $X = +1.2D$ to the value of 30 cm/s which is 10% of the local mean velocity. The turbulence fluctuations at position $X = +2.0D$, $+2.8D$ and $+3.6D$ at the toe side of PVS are the same magnitude as the one at position $X = +1.2D$ (Fig. 6(B)). At the positions $X = +2.8D$ and $+3.6D$, there are double peaks on the u_{rms} profile at toe side. The v_{rms} values show low fluctuation values up to position $X = +1.2D$ and than similar structure with u_{rms} in PVS. The maximum v_{rms} value is 18 cm/s, which is the 6% of local mean velocity. High v_{rms} fluctuation is still detected at the toe side of PVS. The Reynolds stress distribution in the model is shown in Fig. 6(D). The value of the Reynolds stress is zero at the inlet of the model and anastomosis up to position $X = +1.2D$ in PVS. It becomes 818 dynes/cm^2 at position $X = +1.2D$ and then decreases to 300 dynes/cm^2 at position $X = +3.6D$.

3.2. *Systolic peak* ($Re_{60} = 2500$)

Fig. 7(A) shows the vector plot at the systolic peak. Flow enters the model from the graft with a fully developed blunt velocity profile with a centerline velocity of 174 cm/s at position -6.6. Flow enters from the DVS with a fully developed parabolic velocity profile with centerline velocity of 52 cm/s. The flow field changes only slightly from systolic acceleration phase. The separated eddy just downstream of the toe penetrates a bit further into the lumen at position $X = -0.4D$ but reattachment still occurs before position $X = +1.2D$. Further downstream, the profiles generally resembled those found at systolic acceleration except that at position $X = +3.6D$ the u component profile becomes blunt and almost symmetrical. The velocity vectors in PVS are not as parallel as during acceleration as shown in Fig. 7(A). This indicates the strong secondary flow in PVS at this phase angle.

The turbulent fluctuations in both directions are shown by Figs. 8(B)–(C). The u_{rms} profile is "M" shaped. The maximum fluctuation velocity at position $X = -6.6D$ was $u_{rms} = 6.8$ cm/s (4% of local mean velocity u_m) indicating low turbulence levels at the graft inlet. This is lower than that during systolic acceleration even though the instantaneous Reynolds number is greater at the systolic peak. The v_{rms} value in the inlet was almost zero. The turbulence level continues at this low level in the anastomosis up to position $X = +0.4D$. At position $X = +1.2D$, u_{rms} increases to 45 cm/s which is 12% of the local mean velocity. Turbulence fluctuations downstream of position $+1.2$ remain similar in magnitude. At the position $X = +2.8D$ and $+3.6D$, u_{rms} profile has a second peak on the floor side. The v_{rms} values show low fluctuation values up to position $X = +1.2D$ and than a similar structure with u_{rms} distribution in PVS. The maximum v_{rms} value is 27 cm/s which is 7% of

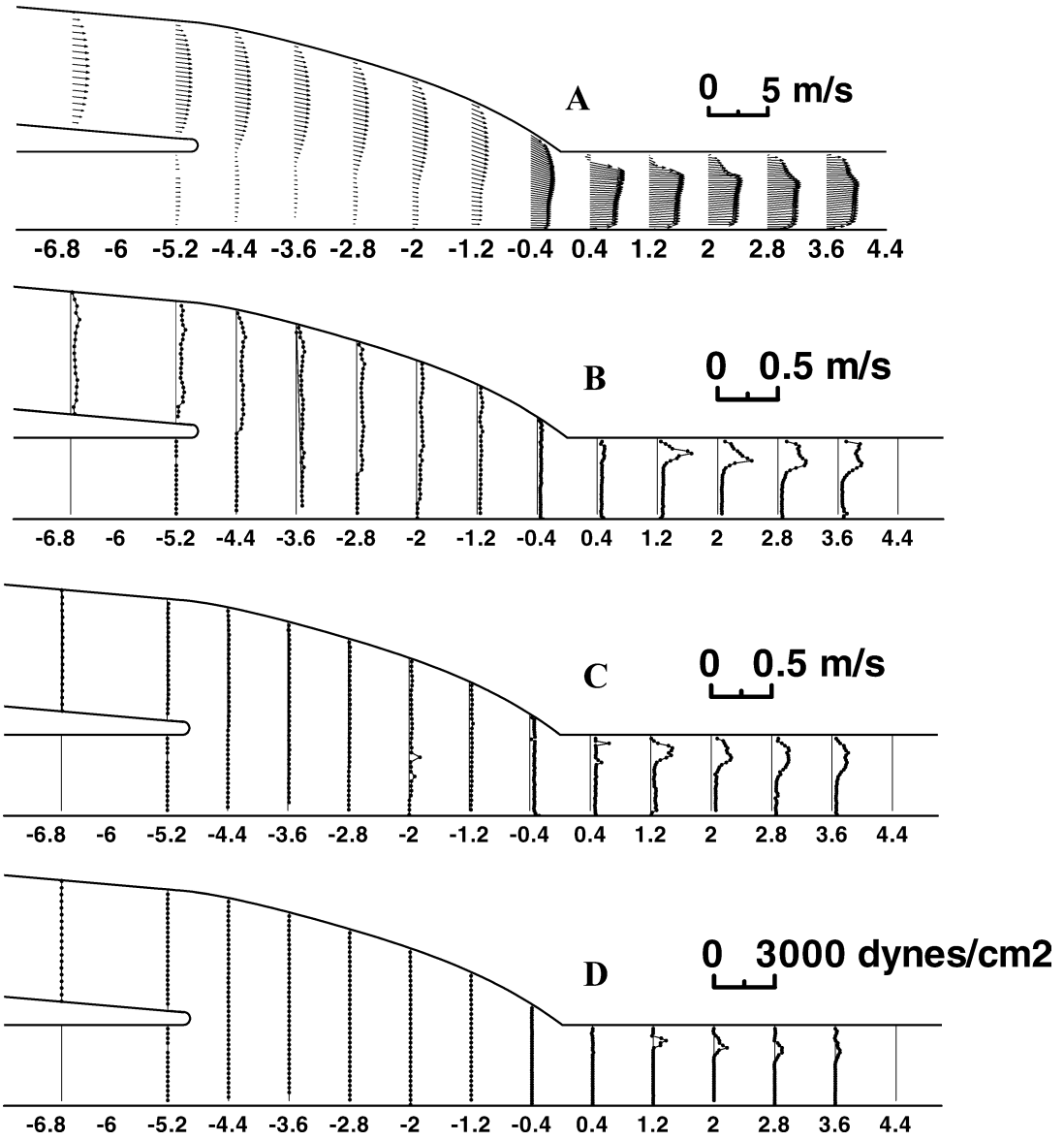

Fig. 6. Vector plots, u_{rms}, v_{rms}, $\rho u'v'$ measured at systolic acceleration.

the local mean velocity. The Reynolds stress distribution in the model is shown in Fig. 7(D). The value of the Reynolds stress is zero at the inlet of the model and anastomosis up to position $X = +0.4D$ in PVS. The maximum value is 1400 dynes/cm^2 at position $X = +1.2D$.

3.3. *Systolic deceleration* ($Re_{120} = 2300$)

Fig. 8(A) shows the velocity vector plot at systolic deceleration. It has a similar velocity field structure as that at systolic peak. Flow enters the model from the graft with a fully developed blunt velocity profile with a centerline velocity of 174 cm/s at position $X = -6.6D$. Flow from DVS with a fully developed parabolic velocity profile enters the anastomosis with a centerline velocity of 62 cm/s. The magnitude of the retrograde vector is smaller than that during the systolic peak while the height is almost the same with. The length of the separation region is almost one diameter. The velocity gradient increases from location $X = +1.2D$ to $+3.6D$ at the toe side of the PVS. The low velocity gradient at the toe side of PVS indicates low WSS at this

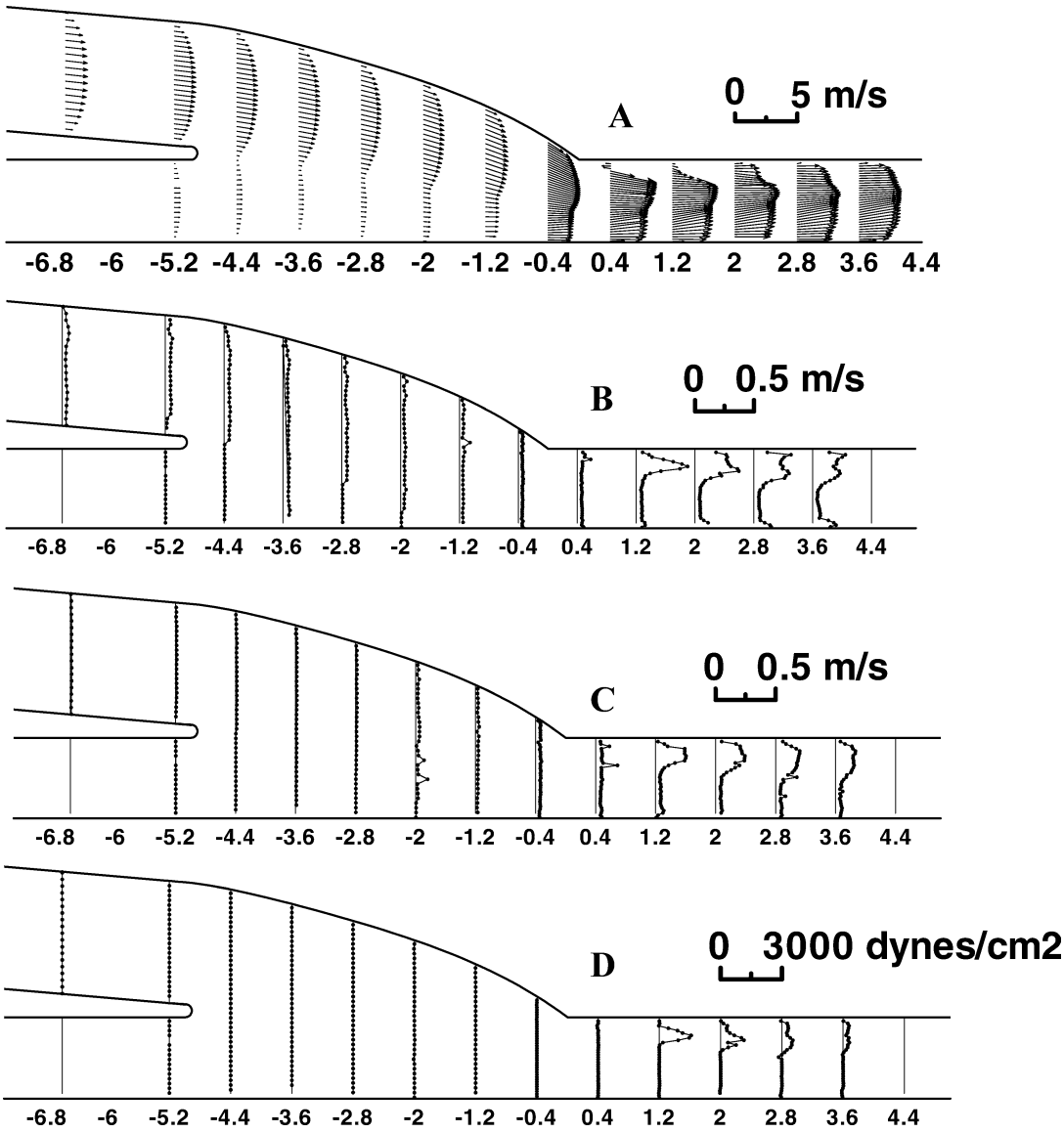

Fig. 7. Vector plots, u_{rms}, v_{rms}, $\rho u'v'$ measured at systolic peak.

side of PVS. The velocity vectors in PVS are towards the toe side. This indicates strong secondary flow in PVS at this phase angle. The velocity gradient on the floor side of position $X = +3.6D$ is less than on the toe side.

The turbulent fluctuations in both directions are given by Figs. 9(B)–(C). The u_{rms} profile is "M" shaped. The maximum fluctuation velocity at position $X = -6.6D$ was $u_{\mathrm{rms}} = 7.8$ cm/s (5% of local mean velocity u_{m}) showing a low turbulence level at the graft inlet. The v_{rms} value was almost zero. The turbulence level is the same order of magnitude inside the anastomosis and up to the location of $X = +0.4D$ in PVS. The v_{rms} increases to 40 cm/s that is the 12% of the local mean velocity at position $+1.2$. The u_{rms} values at position $X = +2.0D$, $+2.8D$ and $+3.6D$ on the toe side of the PVS are the same order of magnitude with that at position $X = +1.2D$. At location $X = +2.8D$ and $+3.6D$, there is double peak on the u_{rms} profile. The v_{rms} values show low fluctuation values up to $X = +0.4D$ and a similar structure as that with u_{rms} in PVS. The maximum v_{rms} value is 25 cm/s, which is 7% of the local mean velocity. High v_{rms} fluctuations are still detected at the toe side of PVS. The Reynolds stress distribution in the model is shown by Fig. 8(D). The value of the Reynolds stress is zero at the inlet of the model and anastomosis up to position $X = +1.2D$ in PVS. It becomes 1167 dynes/cm^2 at position $+1.2$ and then decreases to 327 dynes/cm^2 at position $X = +3.6D$.

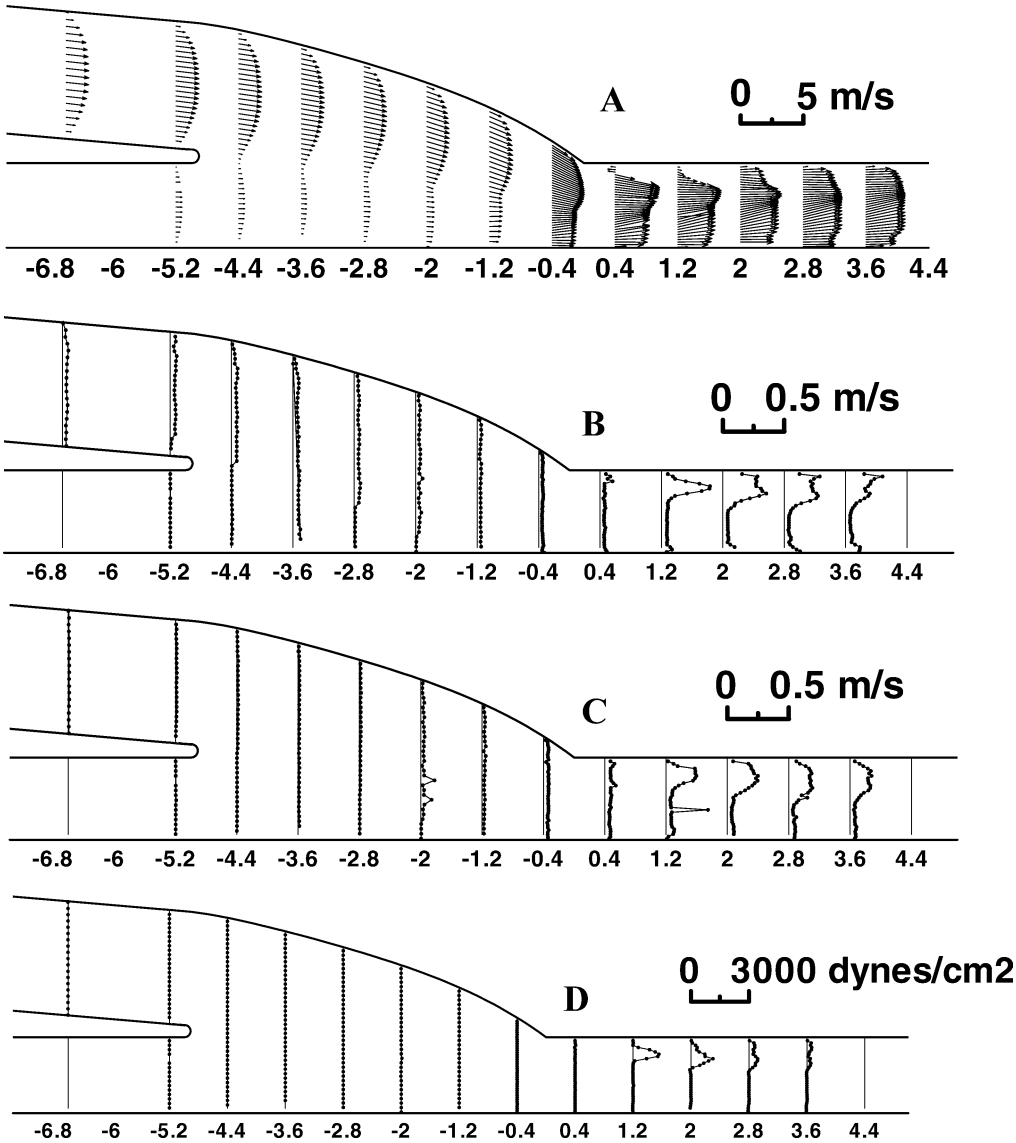

Fig. 8. Vector plots, u_{rms}, v_{rms}, $\rho u'v'$ measured at systolic deceleration.

3.4. *Diastole* ($Re_{300} = 1250$)

Fig. 9(A) shows the vector plot during the diastolic phase. Flow enters the model from the graft with a fully developed blunt velocity profile with a centerline velocity of 87 cm/s at position $X = -6.6D$. Flow from DVS with a fully developed parabolic velocity profile enters the anastomosis with centerline velocity of 22 cm/s. The velocity profiles in the entrance to the PVS are blunt near the floor side and toe side of PVS with high velocity gradients near the walls and the v velocity component increases at the entrance of PVS. The value of the v_{m} increases from 130 cm/s to 217 cm/s at positions of $X = -4.4D$ and $-0.4D$. Again, a separation region downstream of the toe is evidenced by retrograde vectors near the wall at position $X = +0.4D$. The height of the separation region is larger than the one in steady flow. The length of the separation region is almost two diameters. The flow accelerates near the center from 295 cm/s at position $X = +0.4D$ to 304 cm/s at $+2.0D$. This increase in peak velocity is an entrance flow effect. The velocity gradient increases from location $X = +1.2D$ to $+3.6D$ at the toe side of the PVS. The low velocity gradient at the toe side of PVS indicates low WSS at this side of PVS. The velocity vectors in PVS are slightly directed toward the toe side that indicates weak secondary flow in PVS at this phase angle.

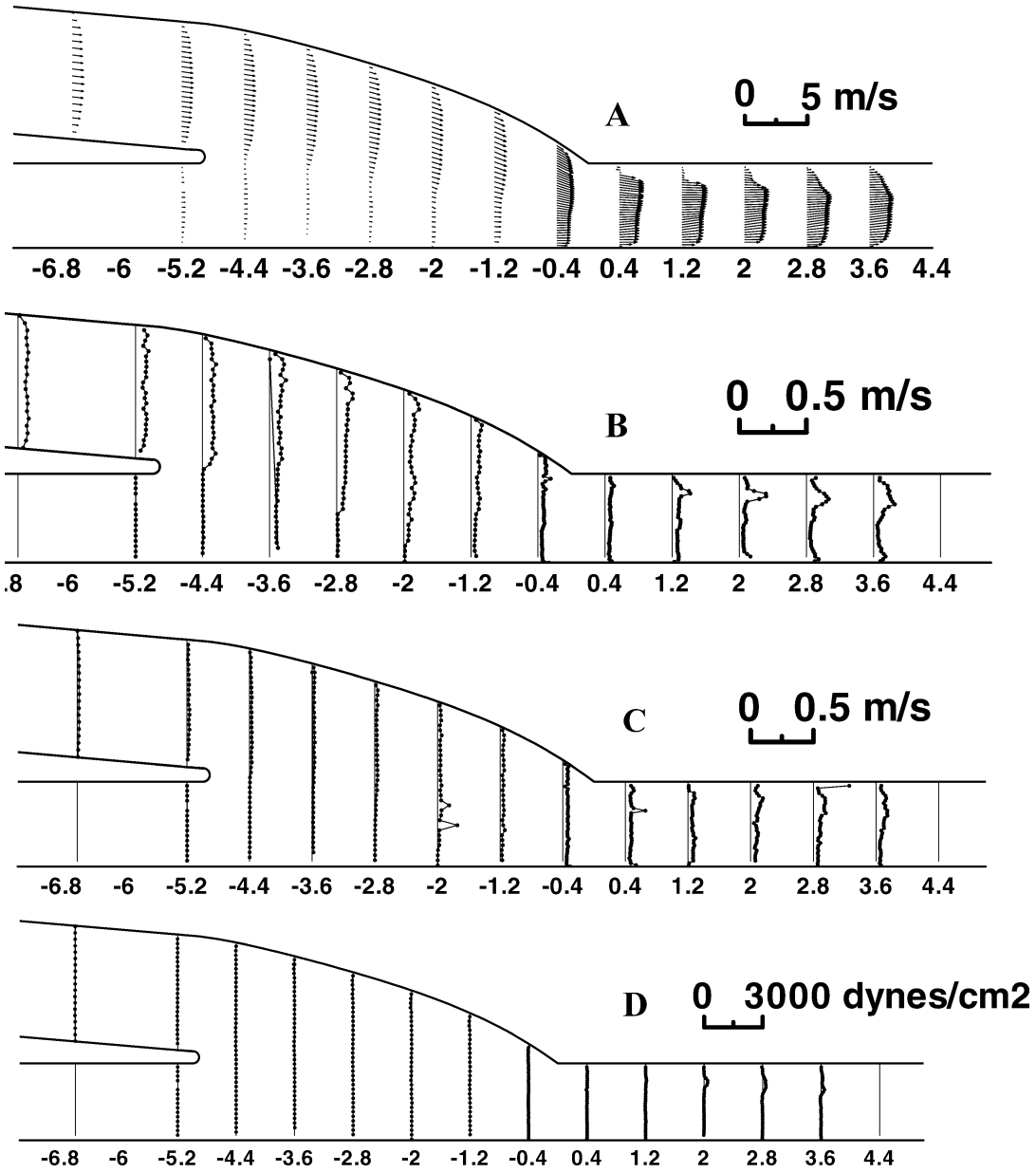

Fig. 9. Vector plots, u_{rms}, v_{rms}, $\rho u'v'$ measured at diastole.

The turbulent fluctuations in both directions are given by Figs. 10(B)–(C). The u_{rms} profile is again "M" shaped. The maximum fluctuation velocity at position -6.6 was $u_{\mathrm{rms}} = 6.5$ cm/s (7% of local mean velocity u_{m}) showing again the low turbulence levels at the graft inlet. The v_{rms} value is zero. The turbulence level is almost same order of magnitude inside the anastomosis up to the location of $X = +1.2D$ in PVS. It suddenly increases to the value of 14 cm/s that is the 30% of the local mean velocity at position $X = +1.2D$. The largest turbulence level is detected at position $X = +2.0D$ as 23 cm/s that is 13% of the local mean velocity. The u_{rms} at positions $X = +2.0D$, $+2.8D$ and $+3.6D$ at the toe side of PVS are the same order of magnitude with that at position $+1.2D$. At the locations $X = +2.0D$, $+2.8D$ and $+3.6D$, there is small second peak the u_{rms} profile at the floor side. The v_{rms} values show low fluctuation values up to position $X = +1.2D$ and than similar structure with u_{rms} in PVS. The maximum v_{rms} value is 11 cm/s that is the 6% of the local mean velocity. The Reynolds stress distribution in the model is shown by Fig. 9(D). The value of the Reynolds stress is zero at the inlet of the model and anastomosis up to

position $X = +1.2D$ in PVS. It becomes 272 dynes/cm^2 at position $X = +1.2D$ and then decreases to 218 dynes/cm^2 at position $+3.6D$.

4. Discussion

The objective of this research was to characterize the flow field within the venous anastomosis of a dialysis patient's AV graft since fluid dynamics has been implicated as a cause of graft failure. The flow field was examined in detail using LDA measurements inside an in vitro model of the venous anastomosis under pulsatile flow conditions. The results of this study show the flow field inside an AV graft to be complex and significantly different than that of an arterial by-pass grafts. The velocity flow field was found to be both laminar and turbulent with a region of a separated flow which created a low WSS region. These velocity flow patterns may contribute to the development and localization of intimal hyperplasia. The values of Reynolds stress were found to be near the level at which hemolysis can occur.

The secondary flow structure is seen visually from vector plots at different phase angles. At systolic acceleration, the velocity vectors are slightly skewed to the toe side of PVS which indicates weak secondary flow. However, at phase angle of 60 degrees, the velocity profile is strongly skewed to the toe side of PVS which shows the strong secondary flow (strong v component of the velocity). The secondary flow continues to be stronger at systolic deceleration and becomes weaker at diastolic phase. The velocity measurements were done at the bifurcation plane and the plane which is perpendicular to the bifurcation plane for steady flow and the secondary flow was discussed in our first steady paper in detail [9].

The experimental model was assumed rigid. We expect the rigid-model assumption to be reasonable because both vein and PTFE have small compliance at these pressures and because the pressure variation in the graft is much lower than that in arteries. The mean and variation in pressure measured in the animal study were 20 and 1mmHg, respectively, versus 100 and 20 mmHg for arteries [9].

The "M" shaped fluctuation velocity profiles were measured at the inlet of the graft at all phase angles. Within the anastomosis, turbulent levels were slightly higher value on the hood side. This is due slightly higher local Reynolds number on the hood side. The highest turbulent level was detected at the toe side of the PVS at all phase angles with the maximum occurring at $X = +1.2D$. The highest velocity fluctuation was 12% of the local maximum mean velocity at the systolic peak at the location of $X = +1.2D$ (see Fig. 7(B)). A second peak on the fluctuation profile was seen at systolic peak and deceleration at the floor side of PVS (see Figs. 7(B) and 8(C)).

In normal arterial flows studied by Loth et al., [5], pulsatility plays an important role, and a quasi-steady flow assumption may not apply. AV graft flows are abnormal in this respect, in that elevated mean flow rate gives rise to a reduced pulsatility index. The steady flow measurements were done in the same in vitro model used in this study experimentally and the results were published together with the numerical calculations [9]. The differences between steady and pulsatile flow velocity field at high Reynolds number: the results show slightly blunt profile for steady flow. This is due to the development necessary for turbulent flows. There was no reverse flow. Velocity profiles were similar in shape under steady and pulsatile flow conditions because of the low pulsatility. Velocity profiles at systolic peak and systolic deceleration were blunter than systolic acceleration and diastole. This can show the flow becoming turbulent. The vector plots show the high velocity gradients at hood and floor side of the anastomosis.

The frequency analysis was not performed for the pulsatile flow case however; it was discussed in our steady flow paper [9] in detail. Since the pulsatility effect is lower we expect that the results under the pulsatile flow case will be similar to the steady flow case. However the magnitude of the turbulence will be lower under the pulsatile flow conditions. We are 100% confident in the RMS and Reynolds stress values presented.

Velocity fluctuations are thought to damage red blood cells (RBC) only when there is a sufficiently high correlation between two orthogonal components, i.e., high "turbulent" or apparent stress $\overline{u'v'}$. These apparent stresses are a result of the mathematical formulation of the Navier–Stokes equations. They arise from the convective terms of the Navier–Stokes equations and as such represent time averaged momentum transport terms. Many biofluid mechanicians interpret these apparent stress terms as physical stresses. and it is only the apparent stresses which have been assumed to cause hemolysis, Kehoe et al., [14].

5. Conclusions

Highly disturbed flow is associated with kinetic energy transfer as evidenced by vessel wall and perivascular tissue vibration. These stresses probably provide the stimulus that initiates and propagates the release of the biological mediators ultimately responsible of intimal hyperplasia formation.

The critical Reynolds stress reported in different studies referenced earlier varies from 2,500 dynes/cm^2 to 30,000 dynes/cm^2, Kehoe et al., [14], Yoganathan et al., [15], Sutera et al., [16]. Since there was no research done on turbulent and Reynolds stress

estimation in AV graft quantitatively up to now. It is difficult to say if Reynolds stress values found in the present research may damage the red blood cells (RBC) in the blood.

Velocity measurements on this model are practical for validation of future numerical solutions to the Navier–Stokes equations on this geometry under transient/turbulent flow conditions. To fully understand the relationship between hemodynamics and graft failure will require further investigation of the flow field inside an AV graft under the possible different flow and geometrical conditions. Numerical solutions to the Navier–Stokes equations may be important in the examination of these different cases due to the relative ease in changing the geometry and flow conditions for computational solutions compared to experimental measurements.

Further studies should be done on AV grafts with the different flow conditions and geometries together with the clinical studies to understand the affect of hemodialysis on intimal hyperplasia formation and graft failure.

References

[1] D.Y. Fei, J.D. Thomas, S.E. Rittgers, The effect of angle and flow rate upon hemodynamics in distal vascular graft anastomoses: a numerical model study, ASME J. Biomech. Engrg. 116 (1994) 331–336.
[2] M. Hofer, G. Rappitsch, K. Perktold, W. Trubel, H. Schima, Numerical study of wall mechanics and fluid dynamics in end-to-side anastomoses and correlation to intimal hyperplasia, J. Biomech. 29 (1996) 1297–1308.
[3] H.M. Crawshaw, W.C. Quist, E. Serrallach, F.W. LoGerfo, Flow disturbance at the distal end-to-side anastomosis, Arch. Surgery 115 (1980) 1280–1284.
[4] D.P. Giddens, C.K. Zarins, S. Glagov, Response of arteries to near-wall fluid dynamics behavior, Appl. Mech. Rev. 43 (1990) S98–S102.
[5] F. Loth, S.A. Jones, D.P. Giddens, H.S. Bassiouny, S. Glagov, C.K. Zarins, Measurements of velocity and wall shear stress inside a PTFE vascular graft model under steady flow conditions, J. Biomech. Engrg. 119 (1997) 187–194.
[6] R.Y. Kanterman, T.M. Vesely, T.K. Pilgram, B.W. Guy, D.W. Windus, D. Picus, Dialysis access grafts: anotomic location of venous stenosis and results of angioplasty, Radiology 195 (1995) 135–139.
[7] M.C. Shu, N.H.C. Hwang, Haemodynamics of angioaccess venous anastomoses, J. Biomedical Engrg. 13 (1991) 103–112.
[8] N. Arslan, Experimental characterization of transitional unsteady flow inside a graft-to-vein junction, Ph.D. thesis, The University of Illinois at Chicago, 1999.
[9] F. Loth, P.F. Fischer, N. Arslan, C.D. Bertram, S.E. Lee, T.J. Royston, R.H. Song, W.E. Shaalan, H.S. Bassiouny, Transitional flow at the venous anastomosis of an arteriovenous graft: Potential activation of the ERK1/2 mechanotransduction pathway, J. Biomech. Engrg. 125 (2003) 49–61.
[10] P.F. Fischer, N.I. Miller, H.M. Tufo, An overlapping Schwarz method for spectral element simulation of three-dimensional incompressible flows, in: P. Bjørstad, M. Luskin (Eds.), Parallel Solutions of Differential Equations, Springer-Verlag, Heidelberg, 2000, pp. 159–181.
[11] M.F. Fillinger, D.B. Kerns, R.A. Schwartz, Hemodynamics and intimal hyperplasia, in: B.G. Sommer, M.L. Henry (Eds.), Vascular Access for Hemodialysis-II, W.L. Gore & Associates and Precept Press, 1990, 1991, pp. 21–51, Chapter 2.
[12] M.F. Fillinger, E.R. Reinitz, R.A. Schwartz, D.E. Resetarits, A.M. Paskanik, C.E. Bredenberg, Beneficial effects of banding on venous intimal-medial hyperplasia in arteriovenous loop grafts, Am. J. Surgery 158 (1989) 87–94.
[13] M.F. Fillinger, E.R. Reinitz, R.A. Schwartz, D.E. Resetarits, A.M. Paskanik, D. Bruch, C.E. Bredenberg, Graft geometry and venous intimal-medial hyperplasia in arteriovenous loop grafts, J. Vascular Surgery 11 (1990) 556–566.
[14] A.B. Kehoe, Coherent and random apparent stresses in periodically unsteady flows, Ph.D. Thesis, Georgia Institute of Technology, Atlanta, 1990.
[15] A.P. Yoganathan, H.W. Sung, Y.R. Woo, M. Jones, In vitro velocity and turbulence measurements in the vicinity of three new mechanical aortic heart valve prostheses: Bjork–Shiley Monostrut, Omni-Carbon, and Duromedics, J. Thorac Cardiovascular Surgery 95 (5) (1988) 929–939.
[16] S.P. Sutera, M.H. Mehrjardi, Deformation and fragmentation of human red blood cells in turbulent shear flow, Biophys. J. 15 (1975) 1–10.